

MUonE実験によるミューオン $g-2$ を 説明可能な $U(1)_{\mu-\tau}$ ゲージボソンの探索

2022/11/8 FPWS2022

東京大学D1 和田淳太郎

Based on Kento Asai, Koichi Hamaguchi, Natsumi Nagata, Shih-Yen Tseng,
and JW Phys. Rev.D **106** 5, L051702 (2022)

MUonE実験 & Muon g-2

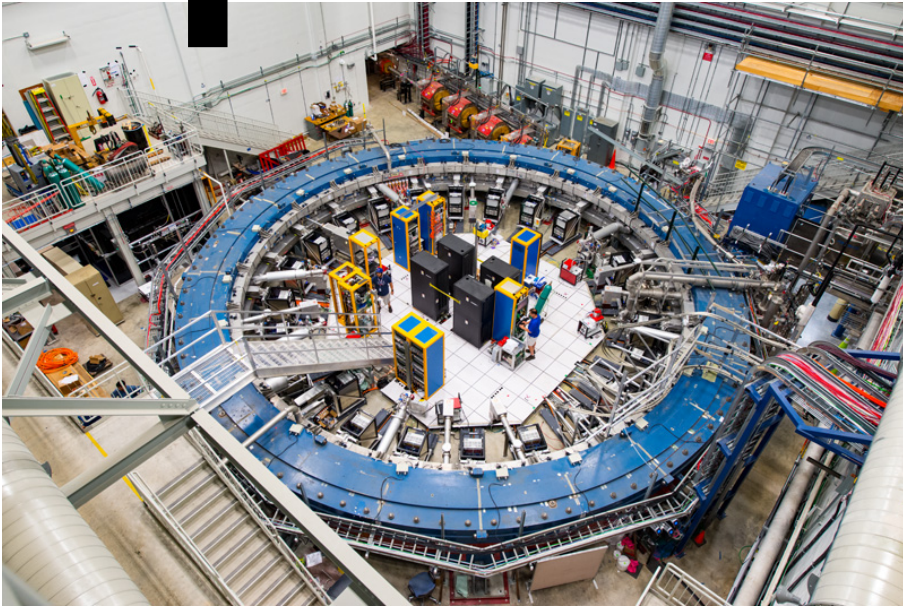
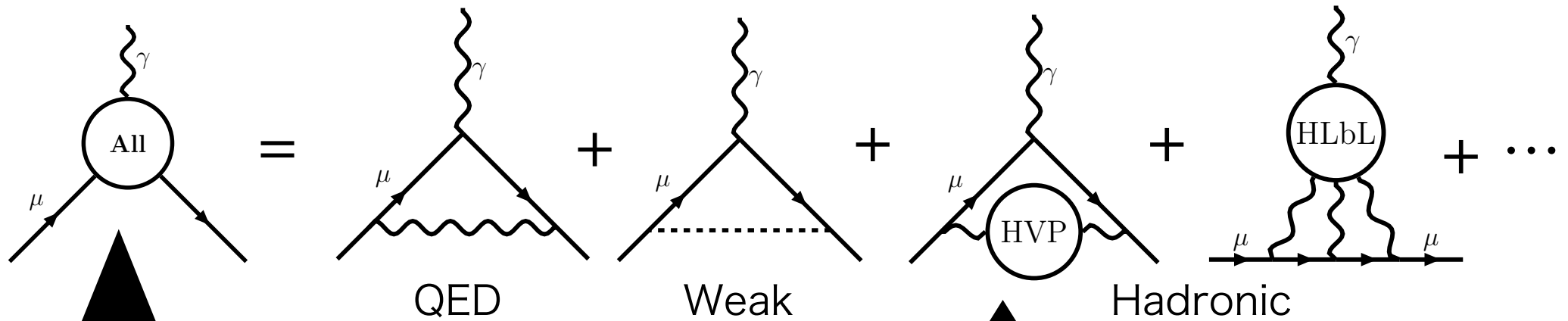
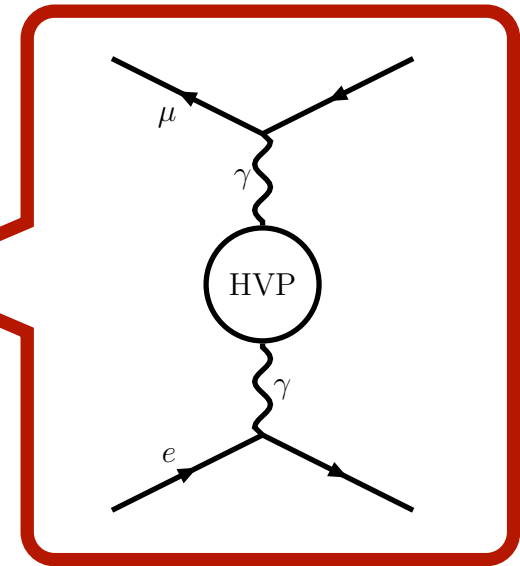


photo from Fermilab Muon g-2 web page

μ ONE



MUonE実験 & Muon g-2

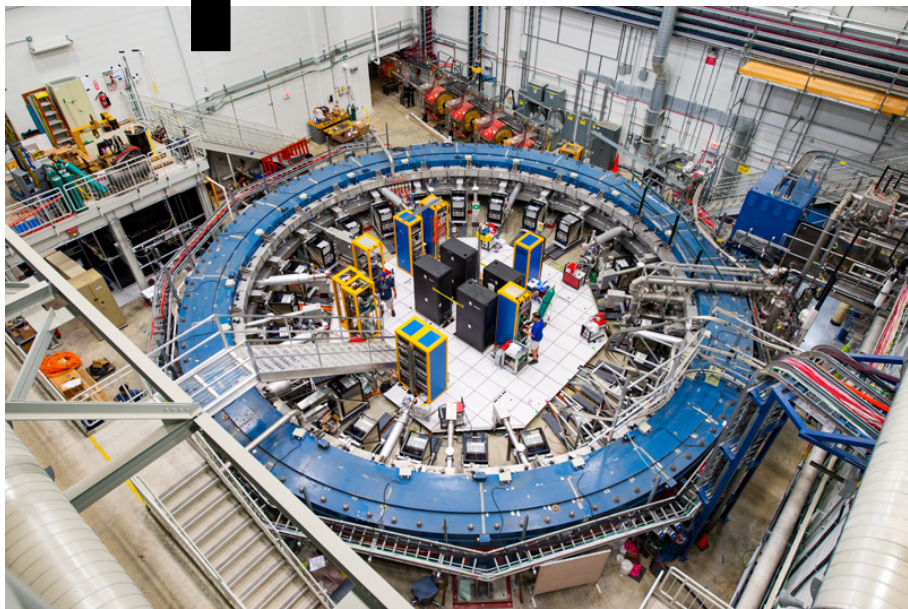
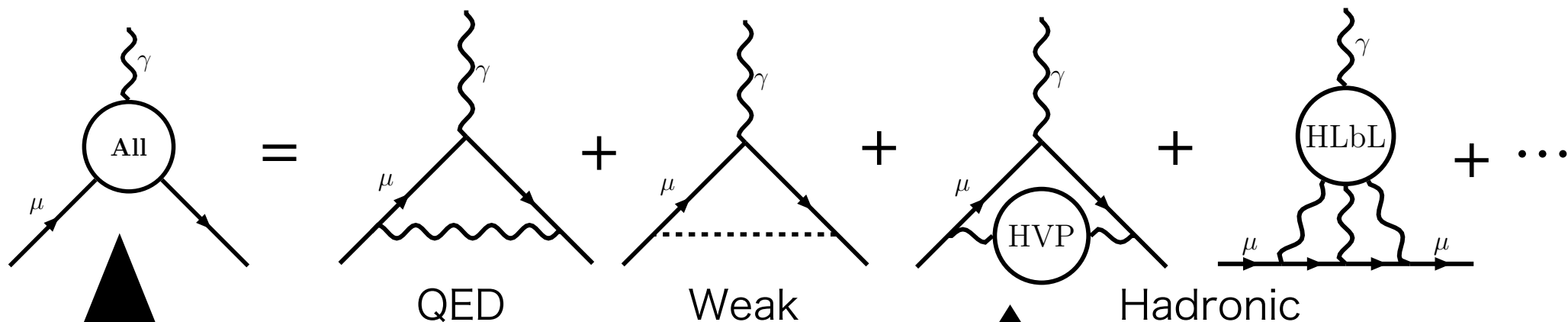
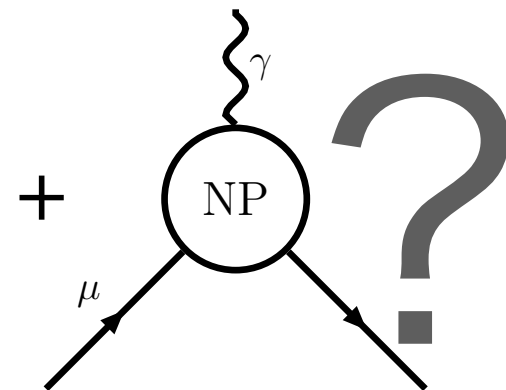


photo from Fermilab Muon g-2 web page



MUonE実験によって
BSMを探れるだろうか？

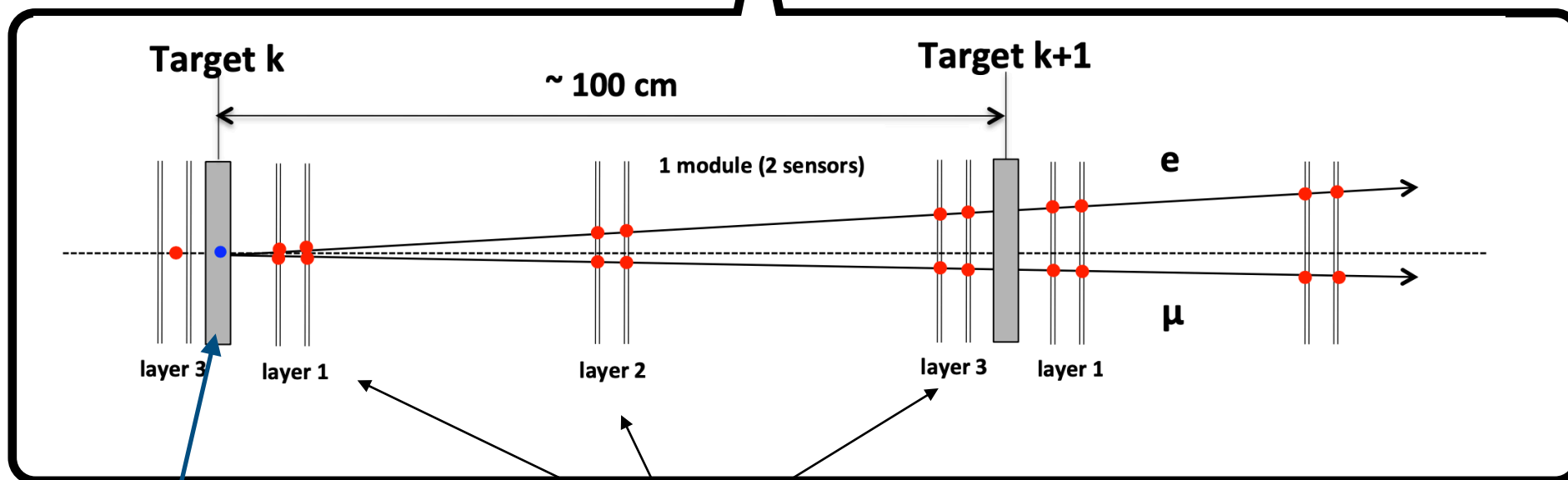
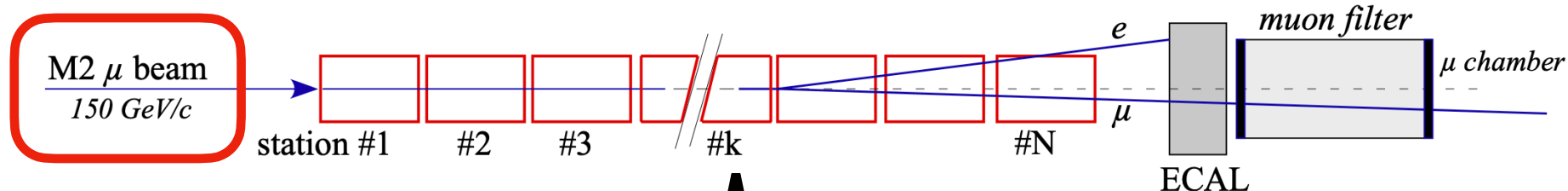
→ $U(1)_{\mu-\tau}$ ゲージボゾン Z' に注目

Outline

- ✓ MUonE実験 & Muon $g-2$
- ▶ MUonE 実験の概要
- ▶ $U(1)_{\mu-\tau}$ ゲージ対称性
- ▶ MUonE 実験と新物理

MUonE実験のsetup

$$\mathcal{L} = 15[\text{fb}^{-1}]$$

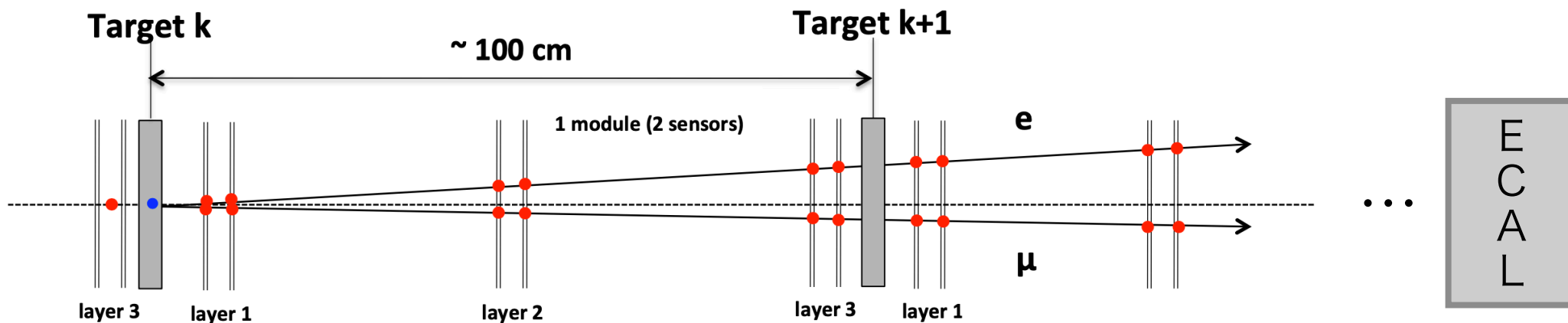
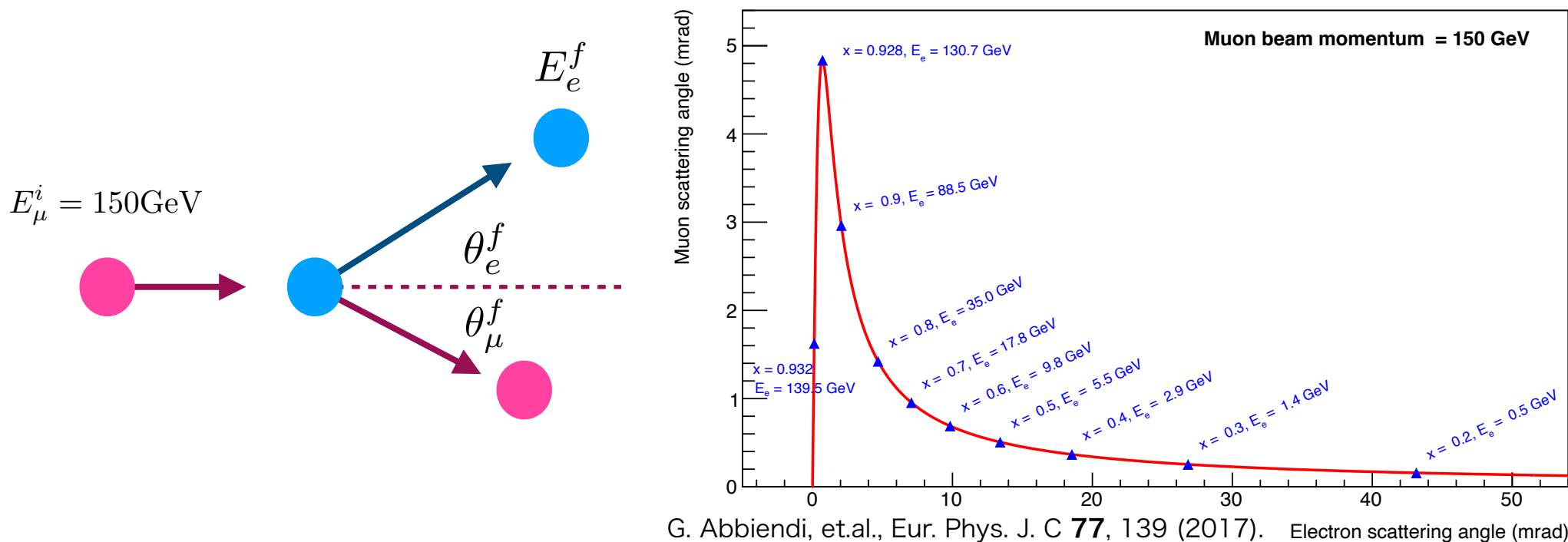


Be target : 15mm

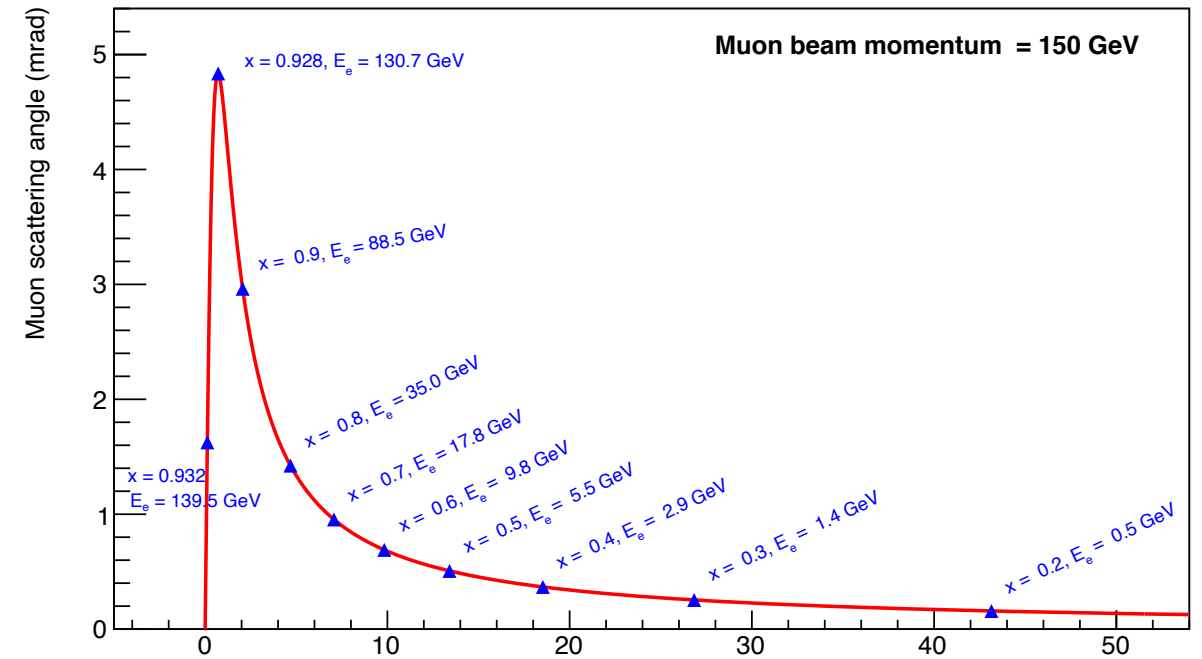
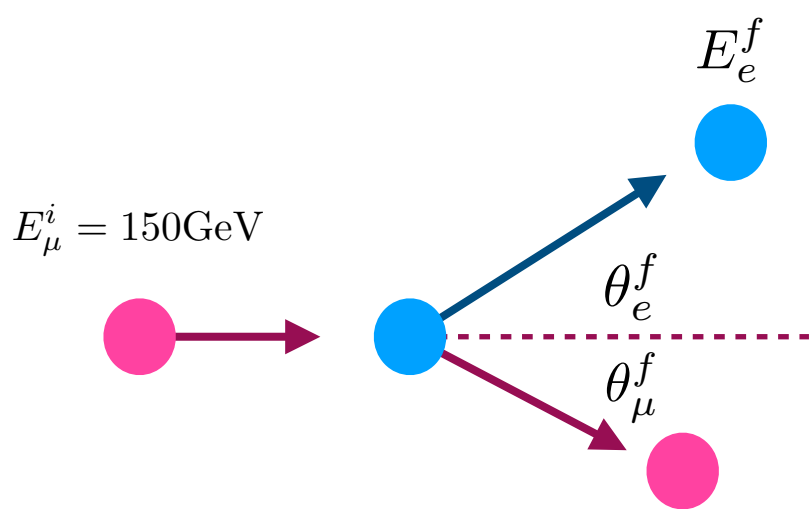
tracker

Angular resolution: $O(0.01)$ mrad expected

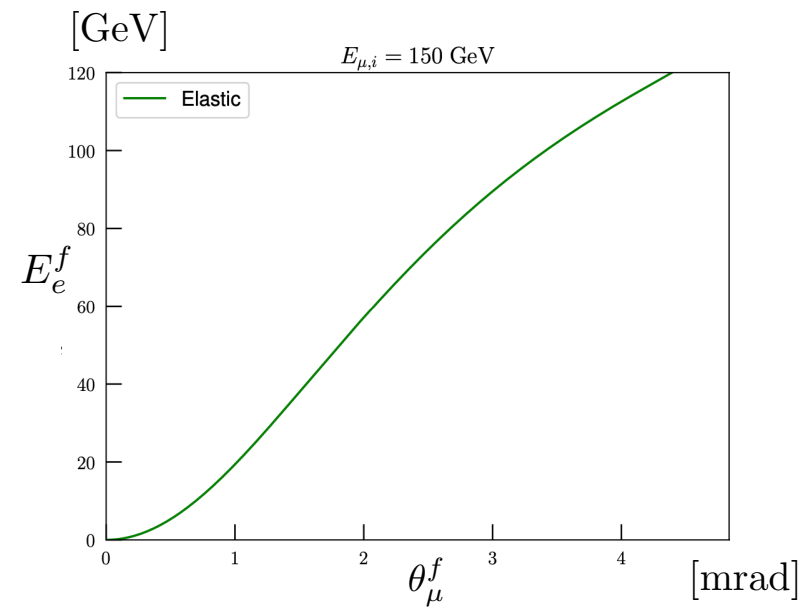
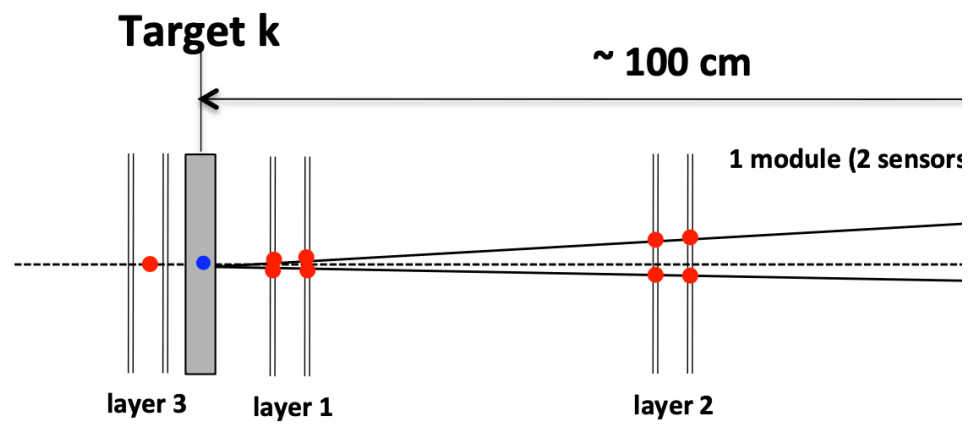
MUonE実験の運動学



MUonE実験の運動学



G. Abbiendi, et.al., Eur. Phys. J. C **77**, 139 (2017). Electron scattering angle (mrad)



E
C
A
L

Outline

- ✓ MUonE実験 & Muon $g-2$
- ✓ MUonE 実験の概要
 - ▶ $U(1)_{\mu-\tau}$ ゲージ対称性
 - ▶ MUonE 実験と新物理

$U(1)_{\mu-\tau}$ ゲージ対称性

$$\mathcal{L} = -\frac{1}{4}F'^{\alpha\beta}F'_{\alpha\beta} + \frac{1}{2}m_{Z'}^2 Z'_\alpha Z'^\alpha + g'Z'_\alpha \sum_{\psi} Q_{\psi} \bar{\psi} \gamma^{\alpha} \psi$$

- ▶ 電子と直接相互作用をしない
- ▶ ゲージアノマリーフリー
- ▶ ニュートリノセクターとの関連

e.g. Neutrino oscillations, Leptogenesis...

Asai, Hamaguchi, Nagata, Eur. Phys. J.C **77** 11, 763 (2017)

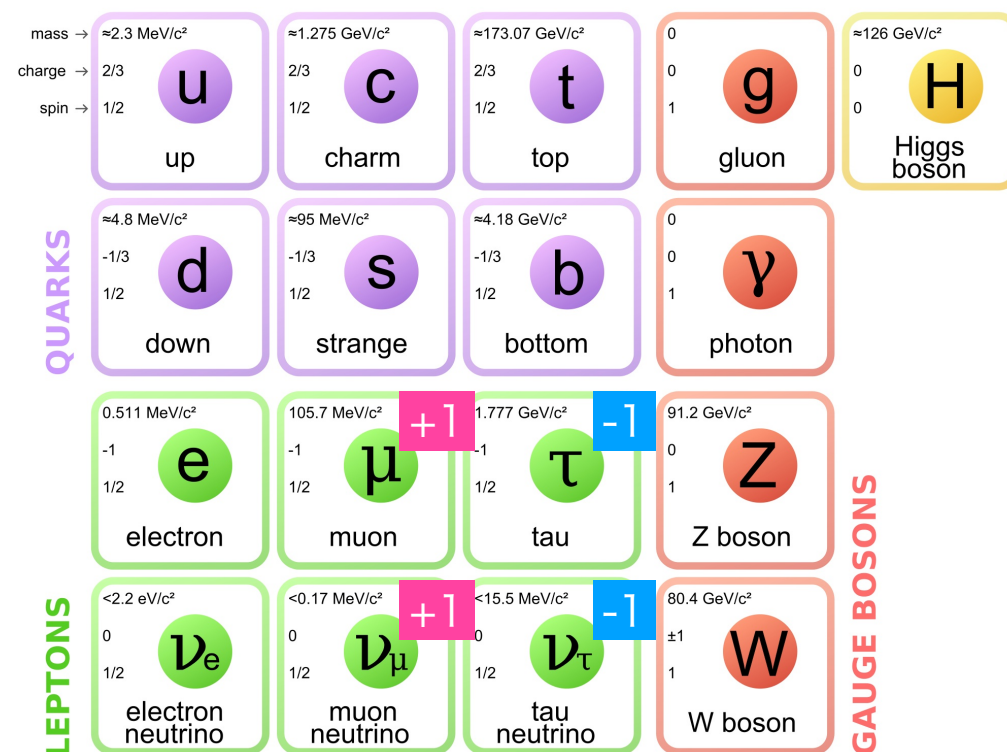
Asai, Hamaguchi, Nagata, Tseng, JCAP **11** 013 (2020)

R. Foot, Mod. Phys. Lett. **A6** 527–530 (1991).

X. G. He, et.al., Phys. Rev. D **43**, 22 (1991).

X. G. He, et.al., Phys. Rev. D **44** 2118–2132 (1991).

R. Foot, Mod, et.al., Phys. Rev. D **50** 4571–4580 (1994).

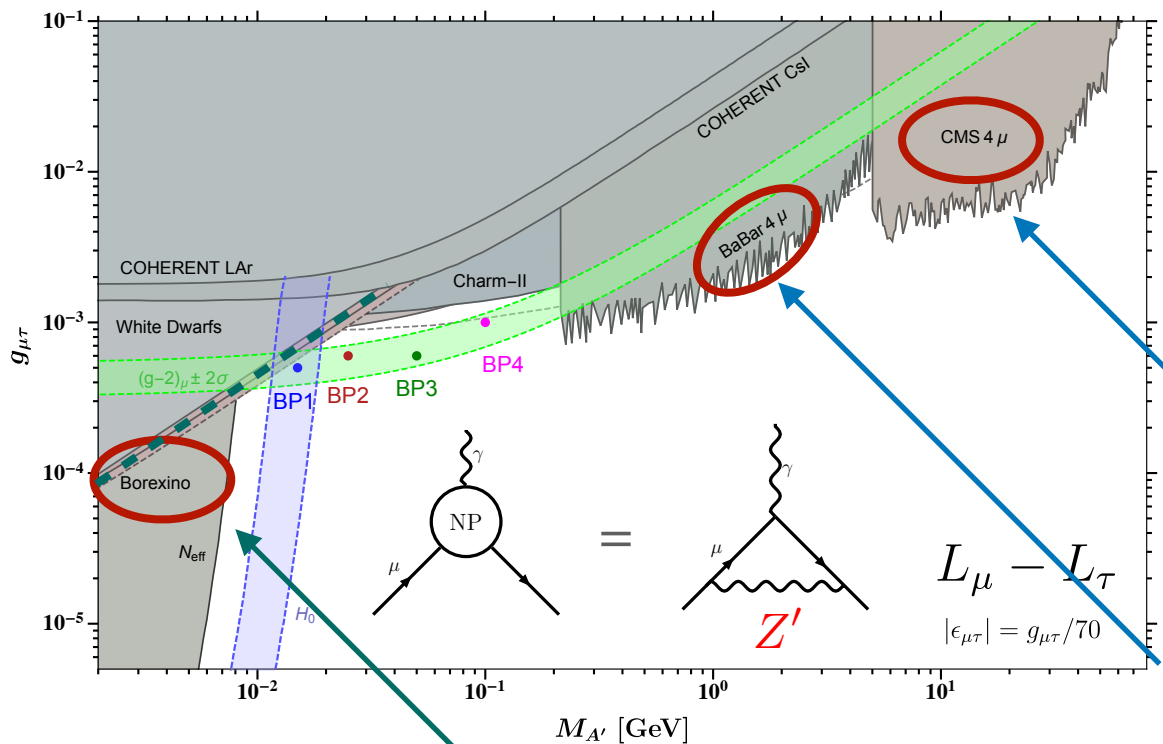


QUANTUM DIARIES

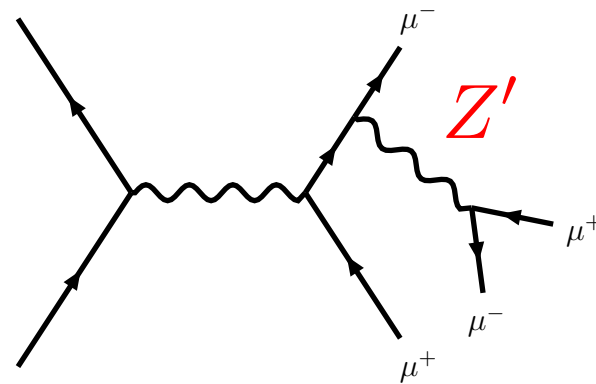
<https://www.quantumdiaries.org/2014/03/14/the-standard-model-a-beautiful-but-flawed-theory/>

+ Z'

実験による制限の現状



D.W.P. Amaral, et al., Eur. Phys. J. C **81**, 861 (2021).



CMS

A. Sirunyan, et al. (CMS) Phys. Lett. B **792**, 345 (2019).

$$q\bar{q} \rightarrow \mu^- \mu^+ Z' \rightarrow \mu^- \mu^+ \mu^- \mu^+$$

BaBar

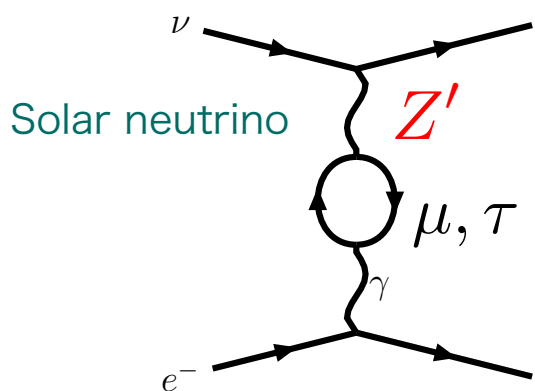
J. P. Lees et al. (BaBar), Phys. Rev. D **94**, 011102 (2016),

$$e^- e^+ \rightarrow \mu^- \mu^+ Z' \rightarrow \mu^- \mu^+ \mu^- \mu^+$$

Borexino

G. Bellini et al. (Borexino), Phys. Rev. Lett. **107**, 141302 (2011)

$$e^- \nu \rightarrow e^- \nu$$



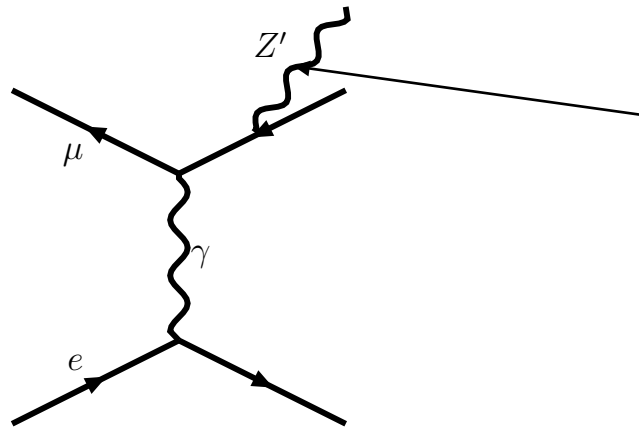
Solar neutrino

Outline

- ✓ MUonE実験 & Muon $g-2$
- ✓ MUonE 実験の概要
- ✓ $U(1)_{\mu-\tau}$ ゲージ対称性
- ▶ MUonE 実験と新物理

MUonE実験と新物理

▶ $\mu e \rightarrow \mu e Z'$ 過程



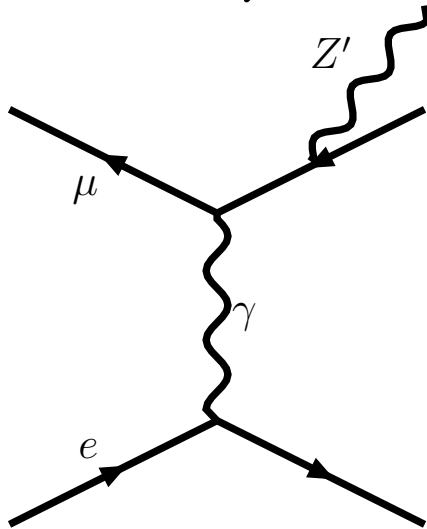
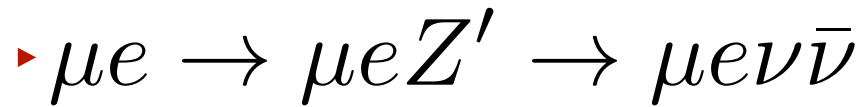
もし、新物理が存在すれば
ゲージボゾン Z' を生成する過程
を捉えられるかもしれない

我々の提案:

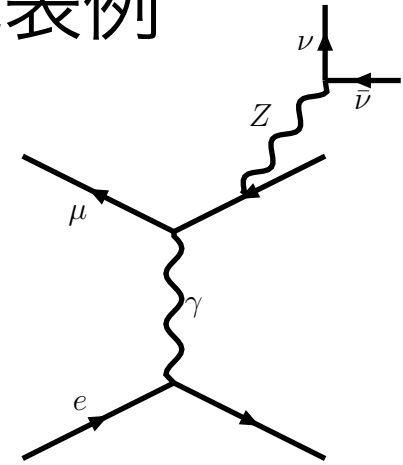
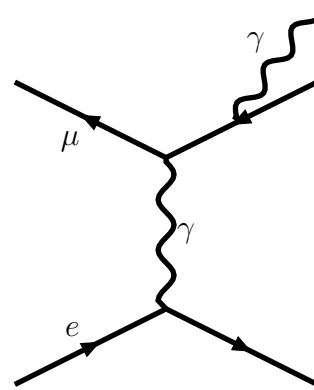
Probing the $L_\mu - L_\tau$ Gauge Boson at the MUonE Experiment

Kento Asai, Koichi Hamaguchi, Natsumi Nagata, Shih-Yen Tseng,
and JW Phys. Rev.D **106** 5, L051702 (2022)

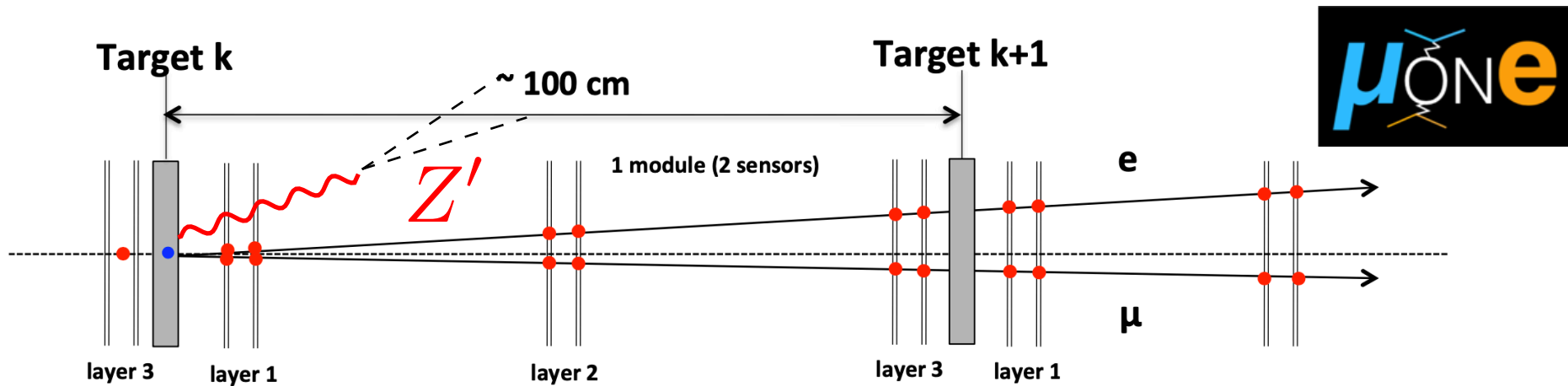
シグナル & バックグラウンド



BG 過程の代表例



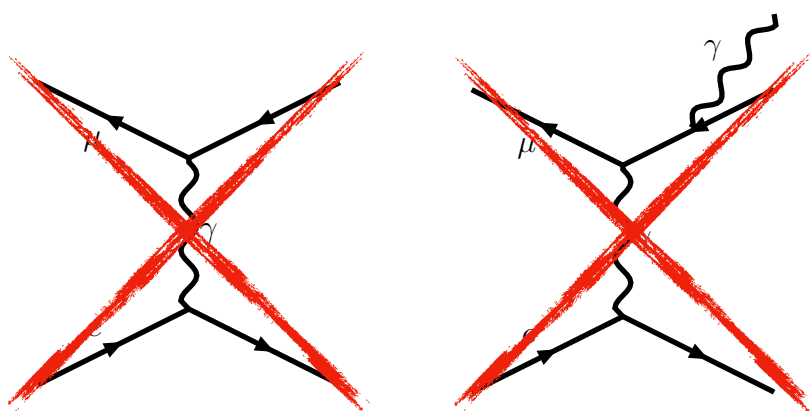
etc...



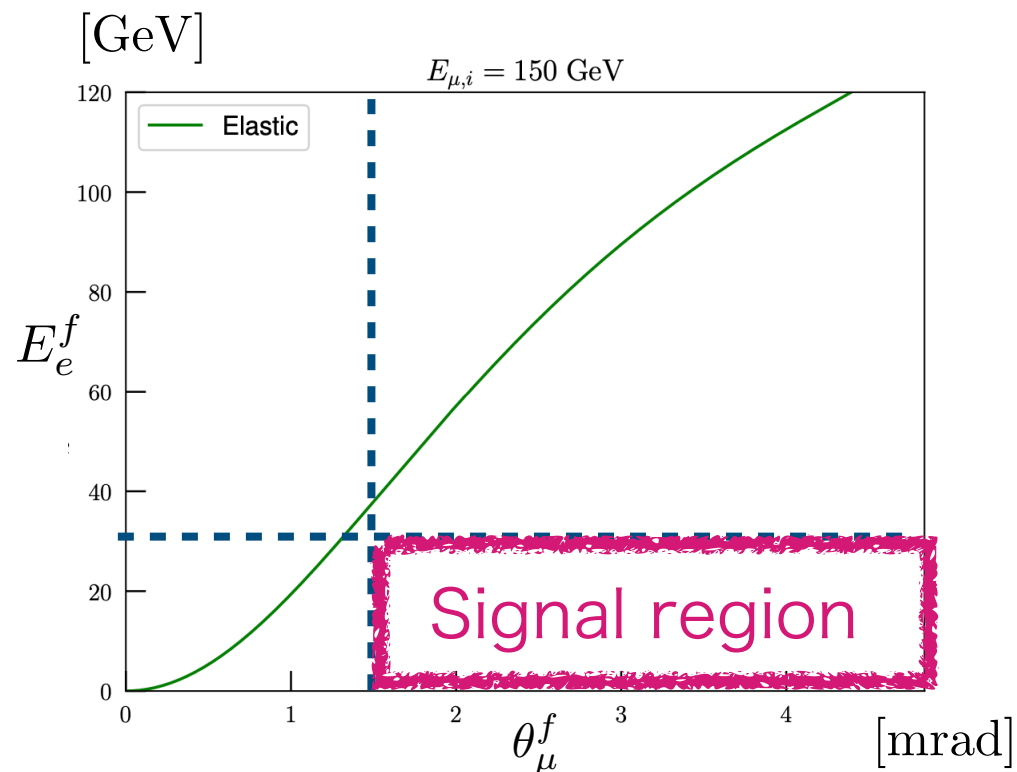
Z' 探索の戦略

以下の選択基準を設定

- ▶ Muon scattering angle
- ▶ Energy of the electron
- ▶ Photon veto



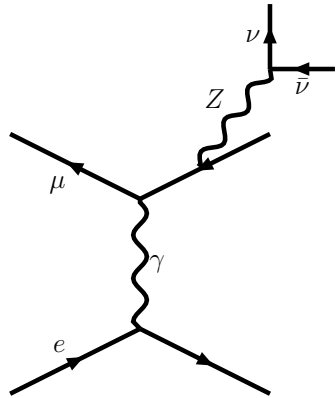
運動学的に排除 + Photon veto



- ▶ $\theta_\mu^f \geq 1.5$ [mrad]
- ▶ $E_e^f \leq 25$ [GeV]

その他のバックグラウンド

- ▶ EW 過程: e.g. $\mu e \rightarrow \mu e Z^* \rightarrow \mu e \nu \bar{\nu}$



MC simulation

▶ $O(10^{-4})$ events

十分無視できる

FeynRules & MadGraph5 _aMC@NLO

N. D. Christensen and C. Duhr,
Comput. Phys. Commun. **180**, 1614 (2009)

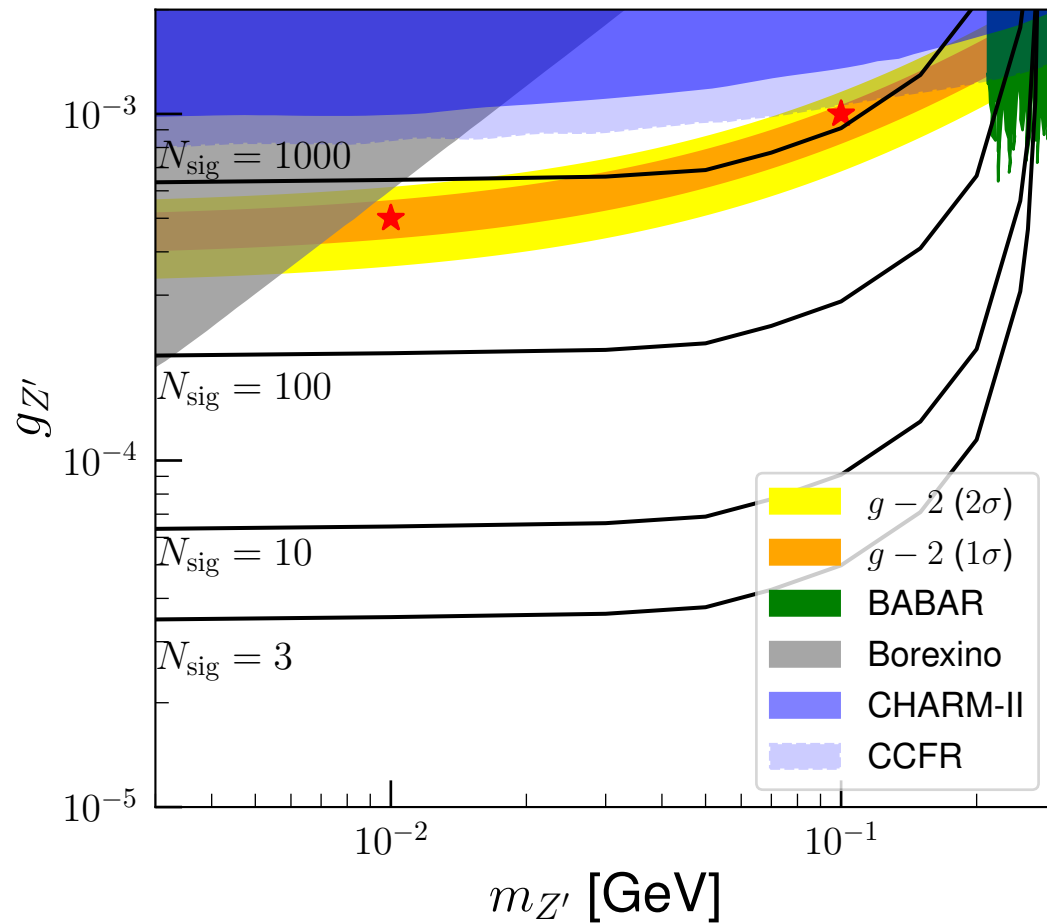
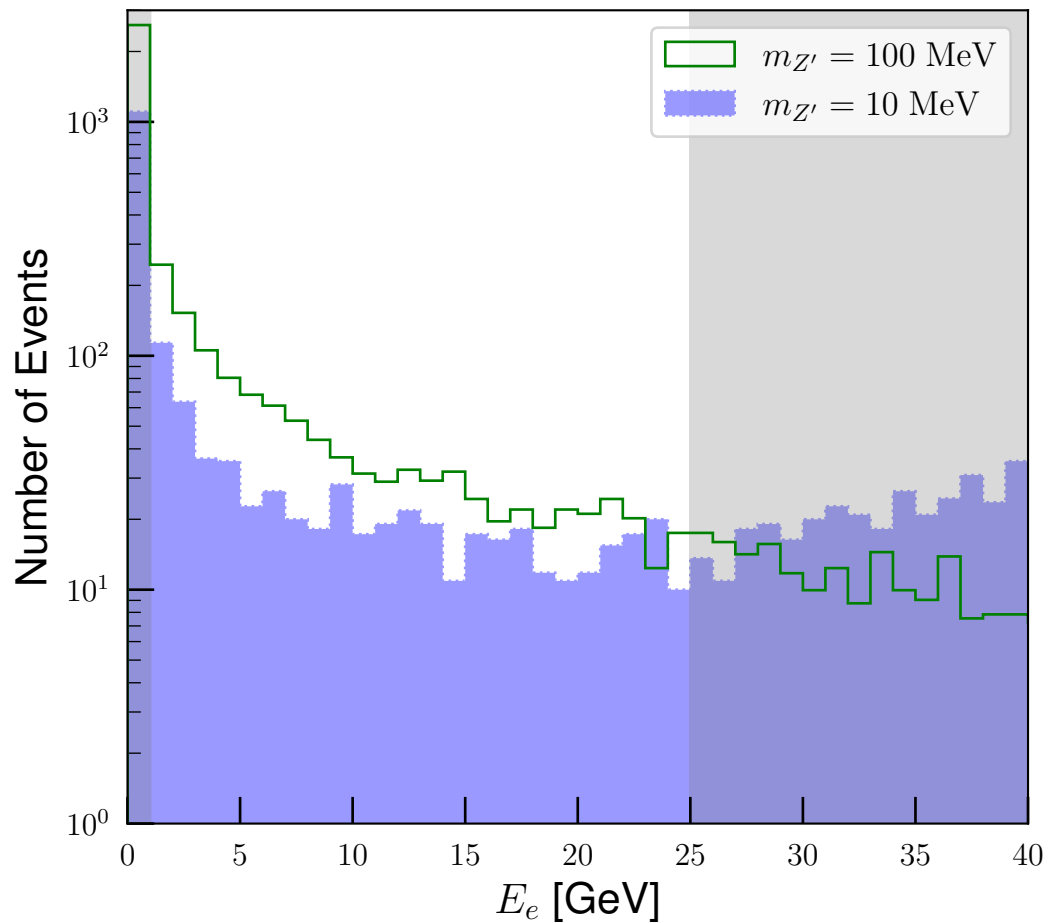
A. Alloul, et.al., Comput. Phys. Commun. **185**, 2250 (2014)

J. Alwall, et.al., JHEP **07**, 079 (2014)

- ▶ 多重散乱
- ➔ トラックーにおけるKink/branch
- ▶ 原子核散乱
- ➔ トラックーにおける粒子多重度

これらの影響は
実験のセットアップに依存
(まだ固定されていない)

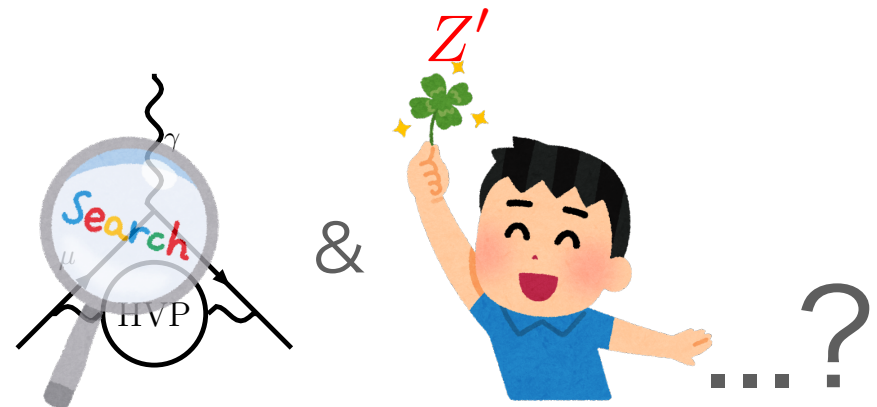
結果



Kento Asai, Koichi Hamaguchi, Natsumi Nagata, Shih-Yen Tseng, and JW
Phys. Rev.D **106** 5, L051702 (2022)

まとめ

- ▶ MUonE実験とは、ミューオン $g-2$ に寄与するHVPの効果をもとに μ - e 散乱を用いることで決定する実験である。
- ▶ 我々は、 $U(1)_{\mu-\tau}$ ゲージボゾン Z' をMUonE実験において運動学的なカットを θ_{μ}^f, E_e^f にかけることで探索できることを示した。
- ▶ 今回の結果は、MUonE実験が新物理にも感度を持つことを表し、故に、MUonE実験は二重の目的を果たすことができる。



Back up

Muon g-2

“White Paper” T. Aoyama, et.al., Phys. Rept. **887**, 1 (2020)

► QED

$$a_\mu(QED) = 116584718.931(104) \times 10^{-11}$$

Smallest error

Up to 5 loops !

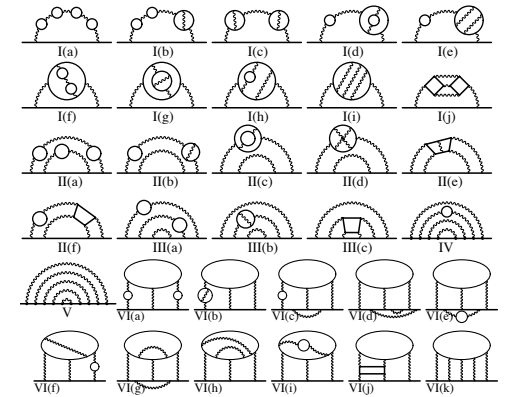
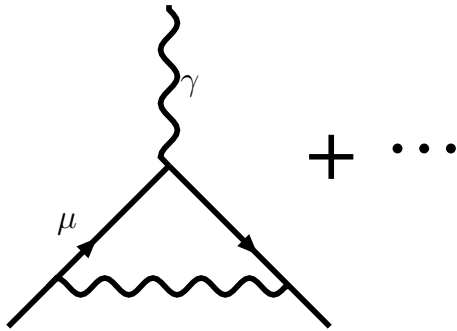


Fig. from 1205.5370

► HVP

$$a_\mu(HVP) = 6845(40) \times 10^{-11}$$

Largest error

(mainly coming from LO)

Using dispersion relation
& experimental data

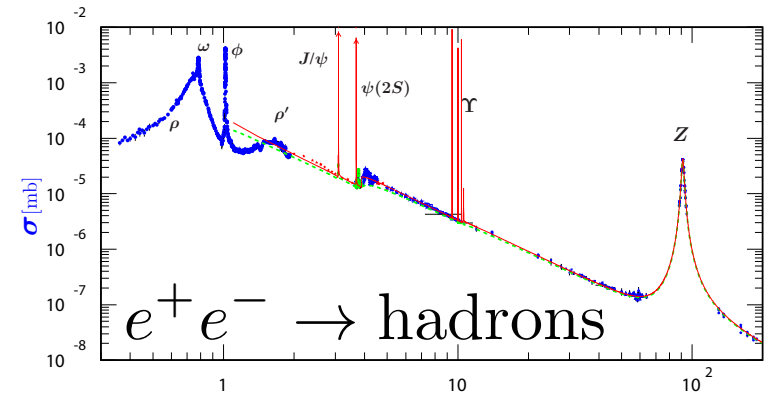
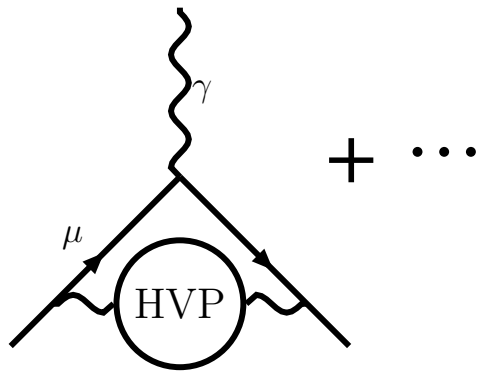


Fig. from PDG

Lattice result

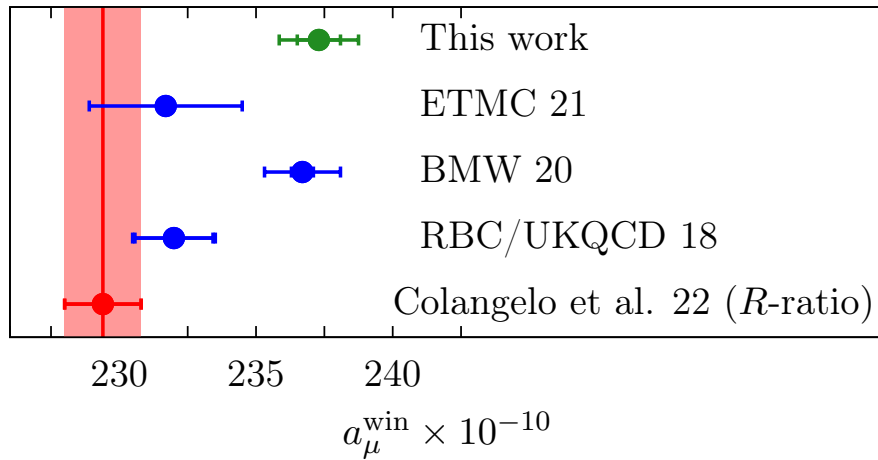


Fig. From M. C`e, et.al., 2206.06582

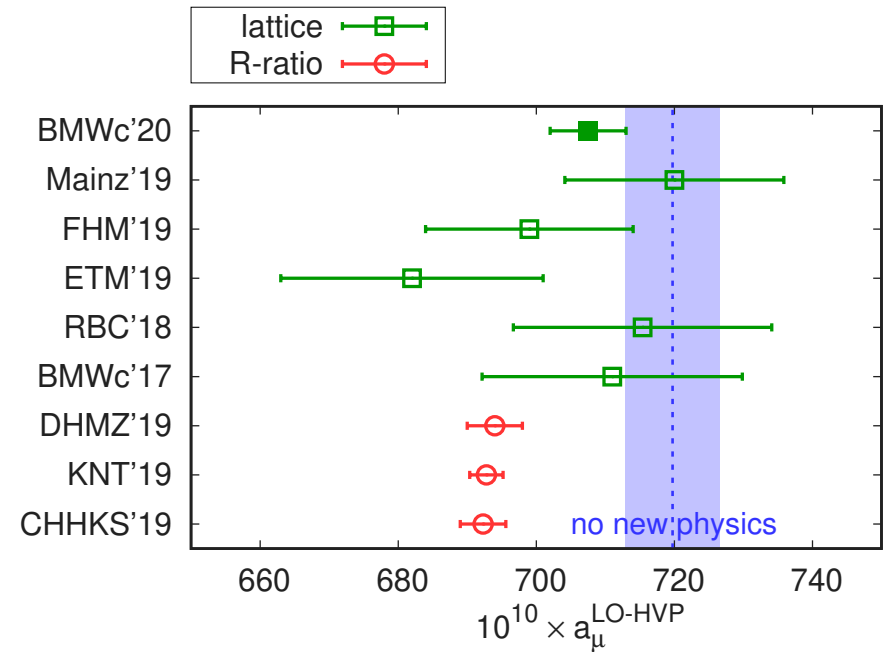
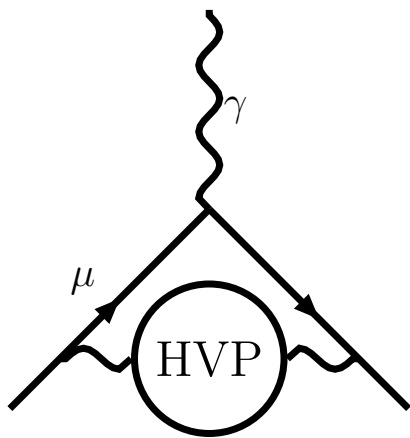


Fig. from S. Borsanyi, et.al., Nature **593**, 51 (2021).



In order to compute HVP...

- ▶ *R*-ratio
- ▶ Lattice

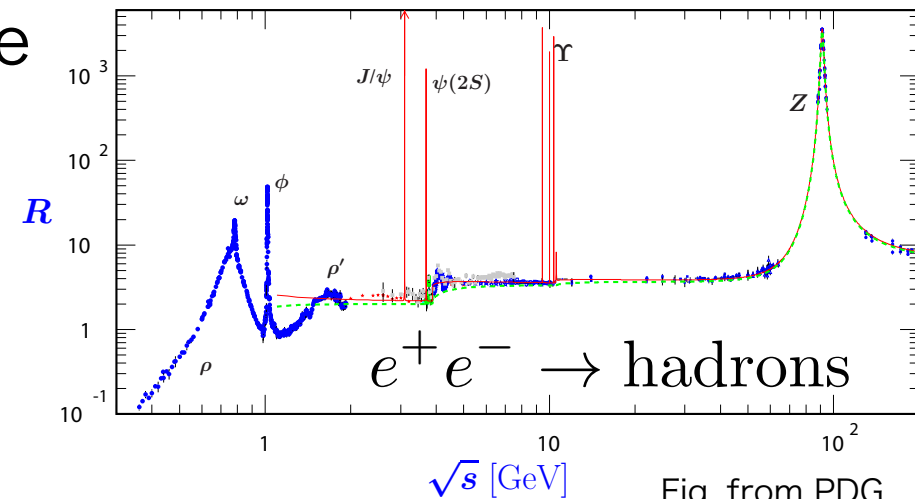
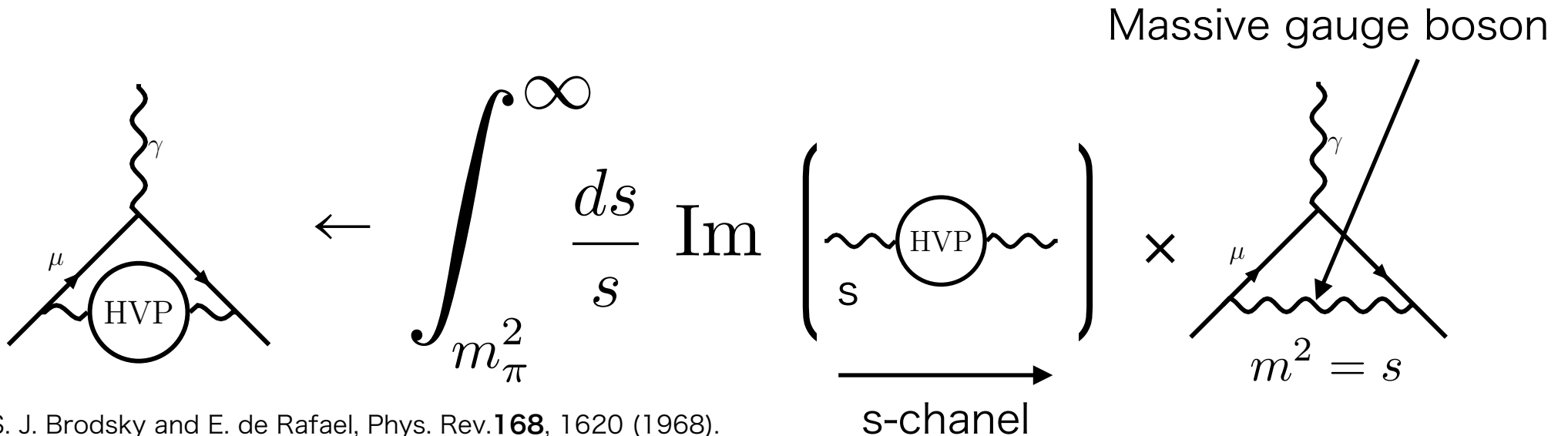


Fig. from PDG

How to calculate HVP?



S. J. Brodsky and E. de Rafael, Phys. Rev. **168**, 1620 (1968).
 M. Gourdin and E. de Rafael, Nucl. Phys. B **10** 667-674 (1969)

In White Paper,
 the authors use this method.

$$\text{Im} \left(\text{HVP} \right) = -\frac{s}{e^2} \left| \text{hadron production} \right|^2$$

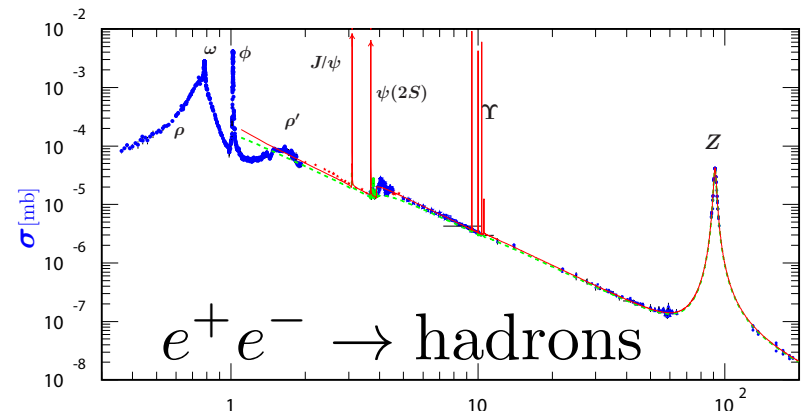


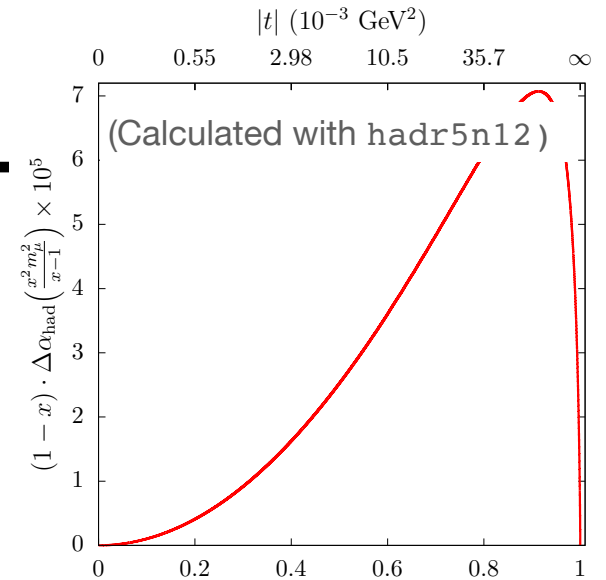
Fig. from PDG

How to calculate HVP?

We can rewrite VP in terms of the effective coupling constant.

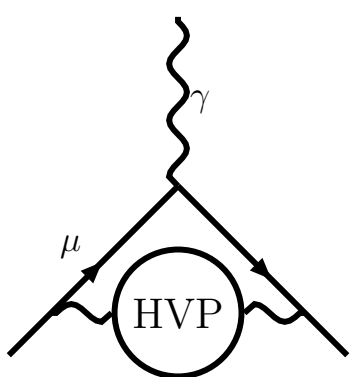
$$\alpha_{\text{eff}}(q^2) = \frac{\alpha}{1 - \Delta\alpha(q^2)} \quad \Delta\alpha \equiv \Pi(q^2) - \Pi(0)$$

Observation value

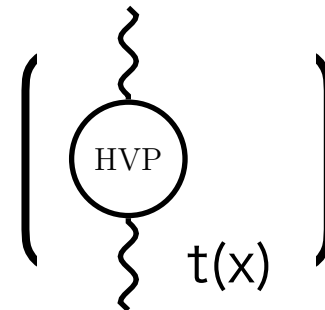


C. M. Carloni Calame, et.al.,
Phys.Lett.B **746** 325-329 (2015).

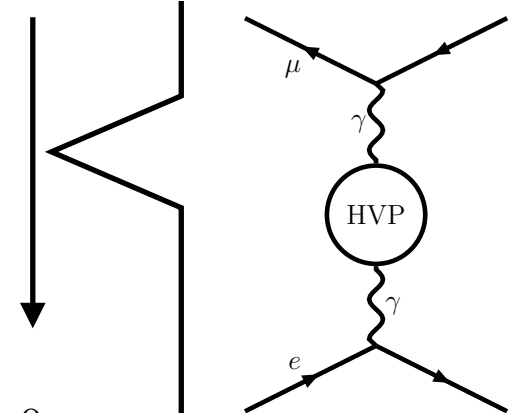
G. Abbiendi, et.al.,
Eur. Phys. J. C **77**, 139 (2017).



$$\int_0^1 dx (1-x)$$



$$t(x) = -\frac{x^2}{1-x} m_\mu^2 < 0$$



t-channel

B. E. Lautrup, et.al., Phys. Rep. **3**, 193 (1972)

HVP error

$$a_\mu(\text{HVP}) = 6845(40) \times 10^{-11} \quad \sqrt{28^2 + 28^2 + 7^2} \simeq 40$$

$$a_\mu^{\text{HVP,LO}} = 6931(28)_{\text{stat}}(28)_{\text{sys}}(7)_{\text{DV+QCD}} \times 10^{-11}$$

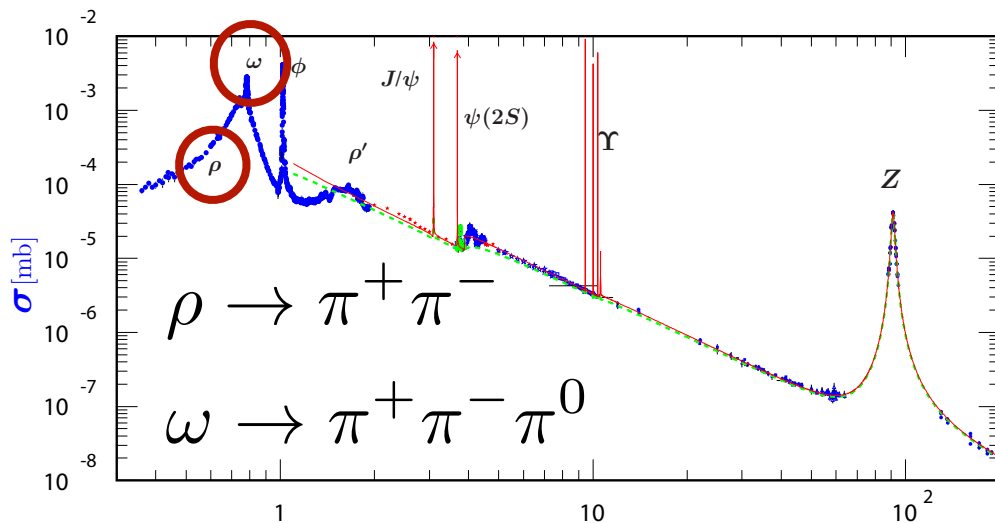
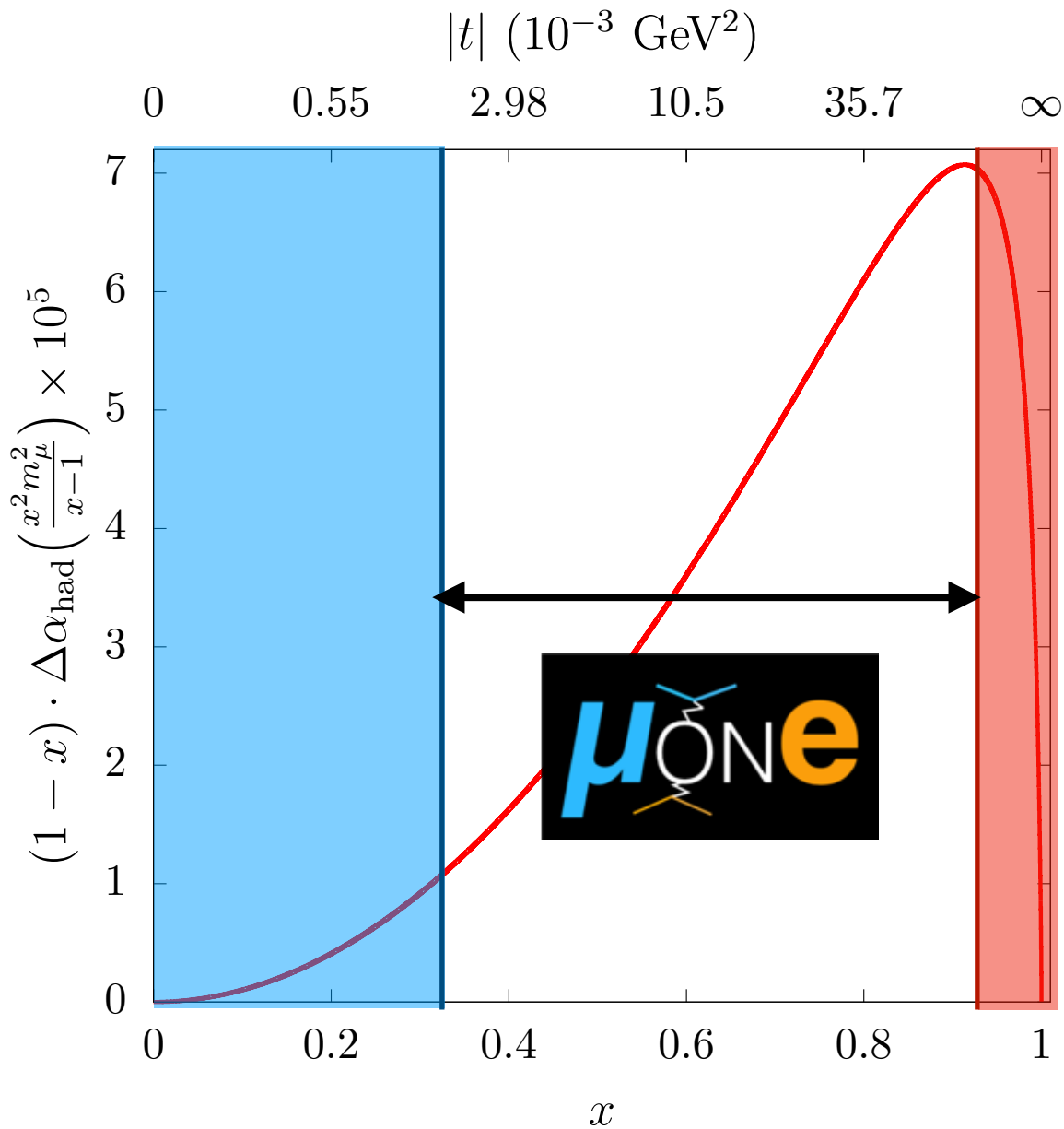


Fig. from PDG

Statistic error mainly come from 2π and 3π channels.

Largest systematic error comes from 2π channel.

MUonE kinematics



$$E_e^f = m_e \frac{1 + \beta^2 \cos^2 \theta_e^f}{1 - \beta^2 \cos^2 \theta_e^f}$$

➔ $1 < E_e^f < 139.8$ [GeV]

Low energy cut: Not fixed yet

$$t = 2m_e^2 - 2m_e E_e^f$$

➔ $-0.143 < t < -0.001$ [GeV]

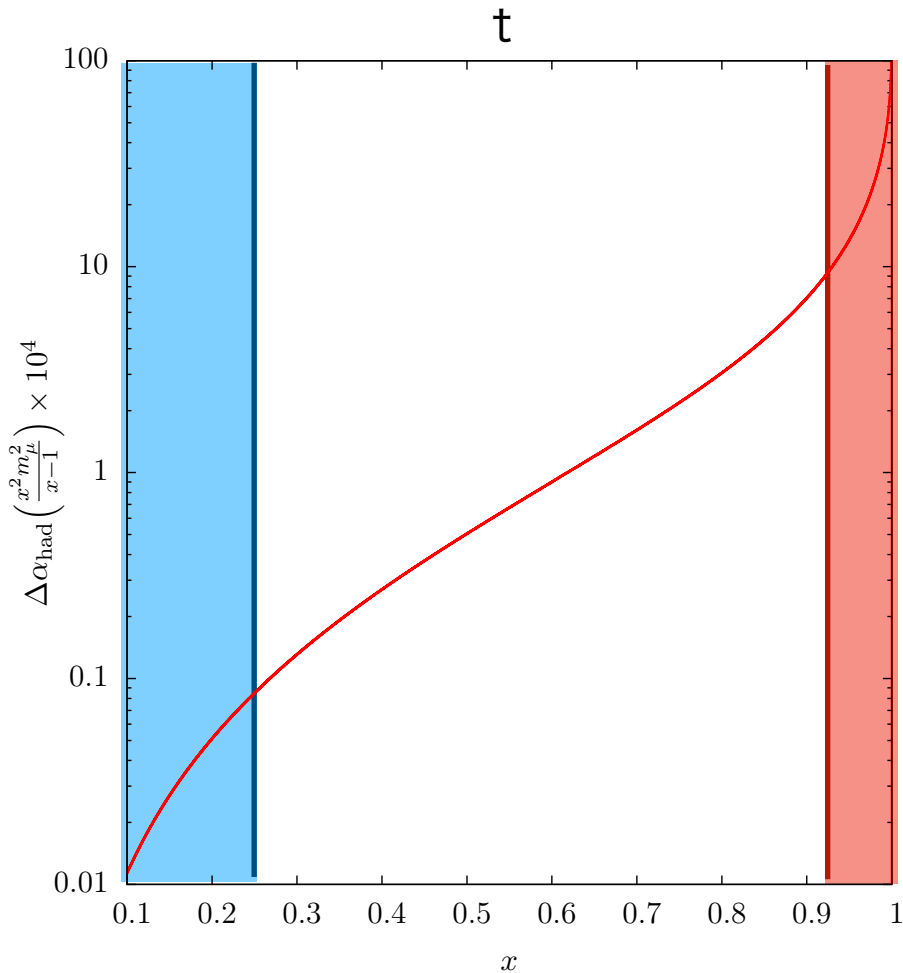
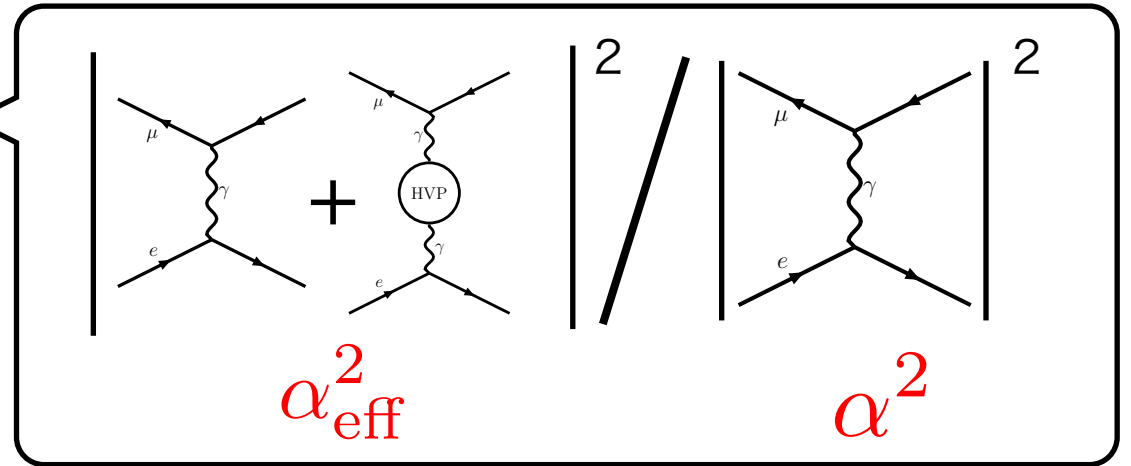
$$t(x) = -\frac{x^2}{1-x} m_\mu^2 < 0$$

G. Abbiendi, et.al., Eur. Phys. J. C **77**, 139 (2017).

MUonE strategy

$$\left(\frac{d\sigma_{\text{had}}}{dt} / \frac{d\sigma_0}{dt} \right) \simeq 1 + 2\Delta\alpha_{\text{had}}$$

$$\alpha_{\text{eff}} = \frac{\alpha}{1 - \Delta\alpha}$$



Divide “t” into bins labeled by “i” and determine $\Delta\alpha_{\text{had}}$ bin by bin

$$\sigma_i \equiv \int_i dt \frac{d\sigma}{dt}(t) \quad \begin{array}{l} \sigma: \text{full cross section} \\ i: \text{the } i\text{-th } t\text{-bin} \end{array}$$

$$\sigma_i = \underbrace{\sigma_{0,i}}_{\text{Computable}} [1 + 2\Delta\alpha_{\text{had},i} + \underbrace{\delta_{\text{SM},i}}_{\text{Computable}}]$$

A report of the MUonE theory initiative

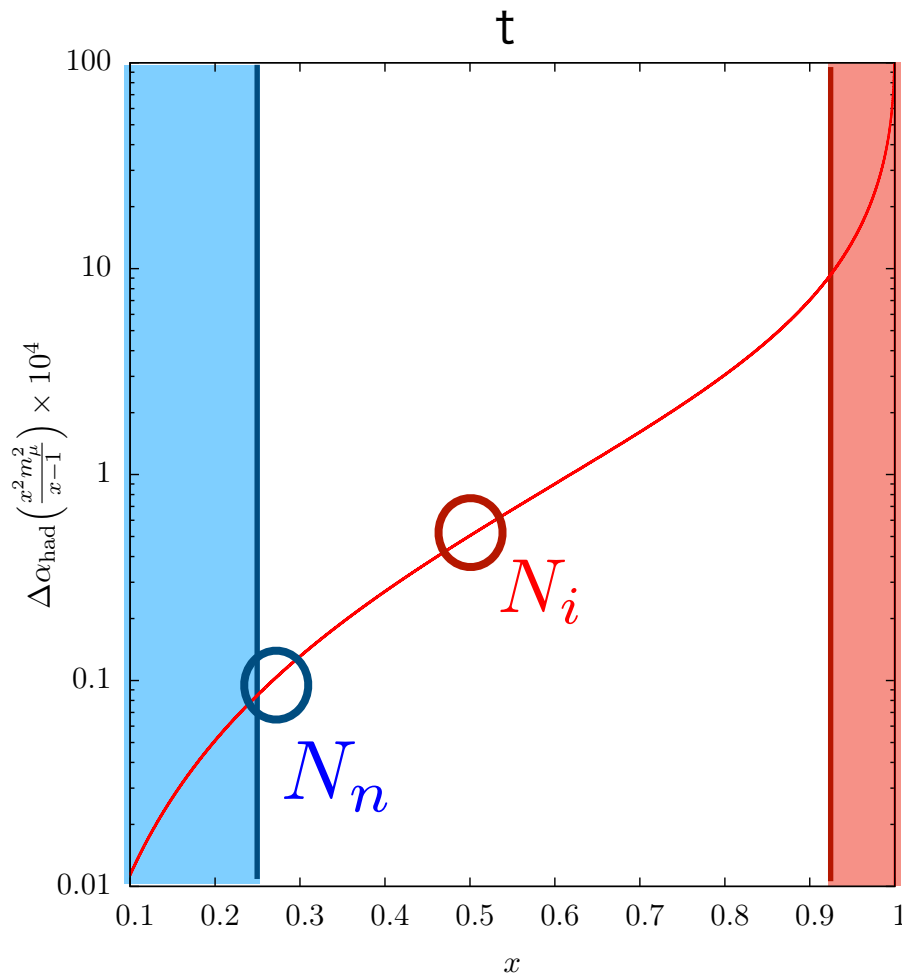
P. Banerjee, et.al., Eur. Phys. J. C **80** (2020) 6, 591

MUonE strategy

Observation value:
event number N_i



We can extract the information
of $\Delta\alpha_{\text{had}}$ from N_i/N_n
(Independent on the luminosity)



$$\frac{N_i}{N_n} \simeq \frac{\sigma_{0,i}}{\sigma_{0,n}} \left[1 + 2(\Delta\alpha_{\text{had},i} - \Delta\alpha_{\text{had},n}) \right]$$

Computable + $\delta_{SM,i} - \delta_{SM,n}$

Computable

$\Delta\alpha_{\text{had},n}$ can be determined by
the time-like data.

MUonE sensitivity

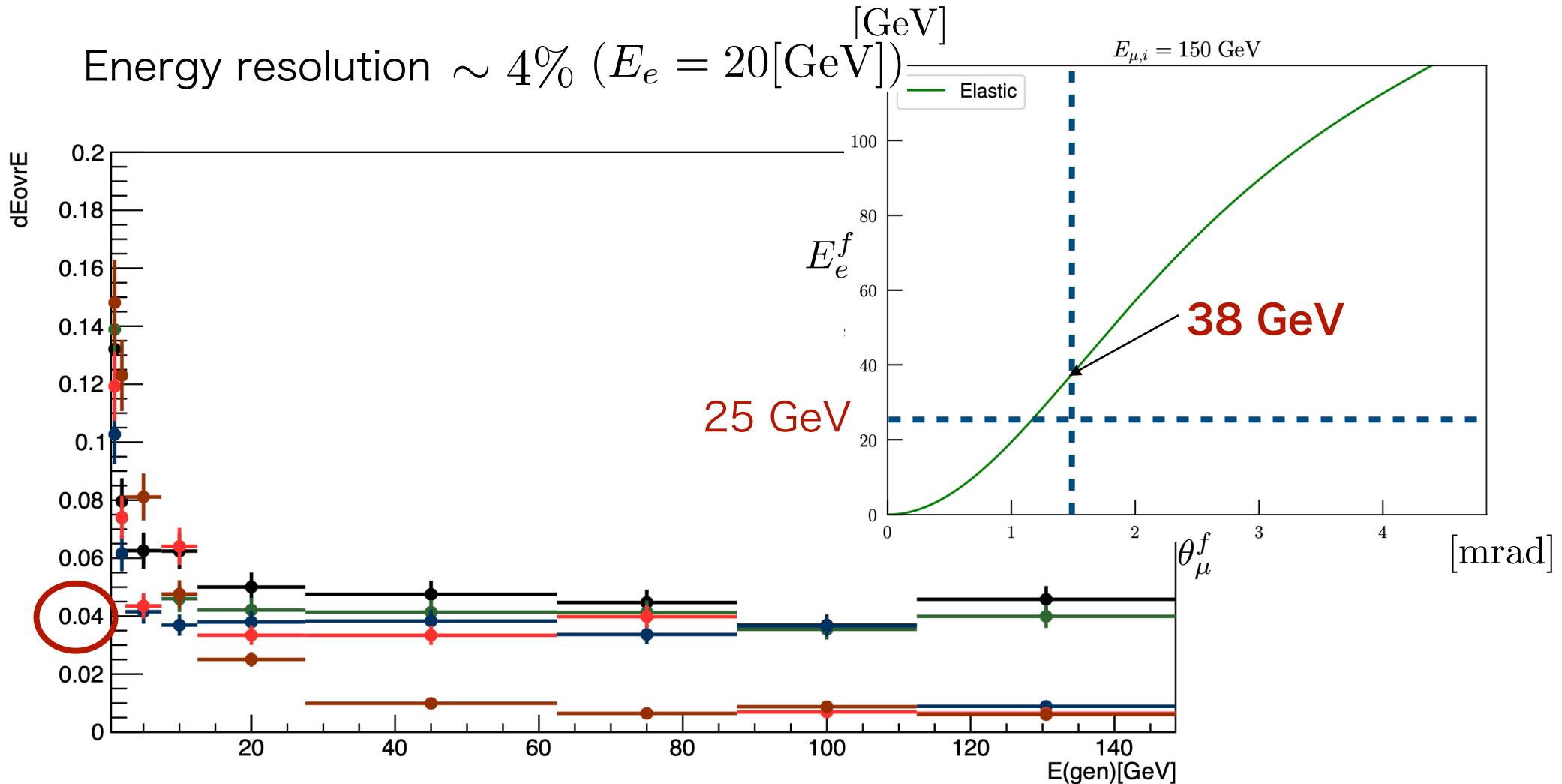
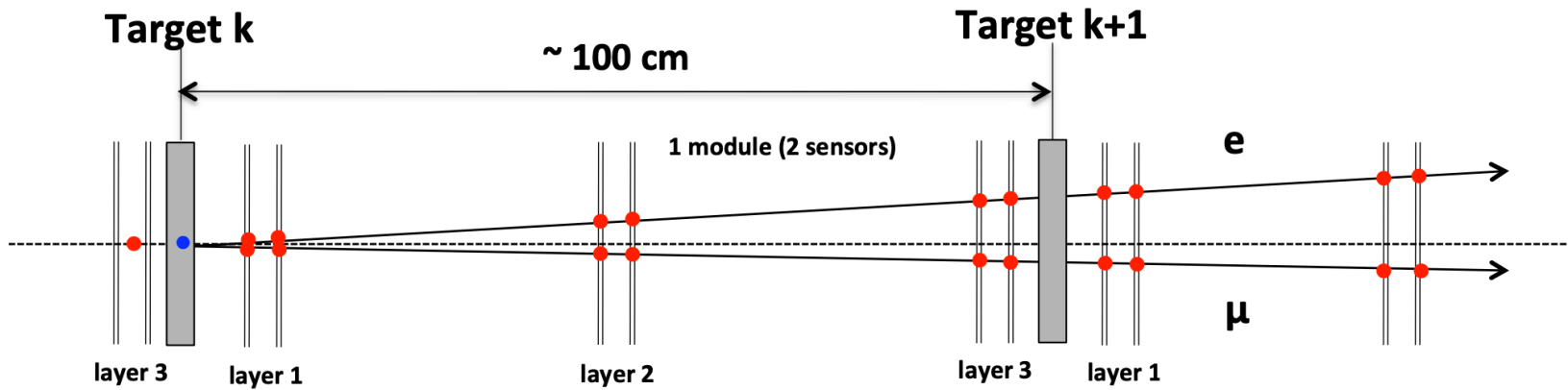
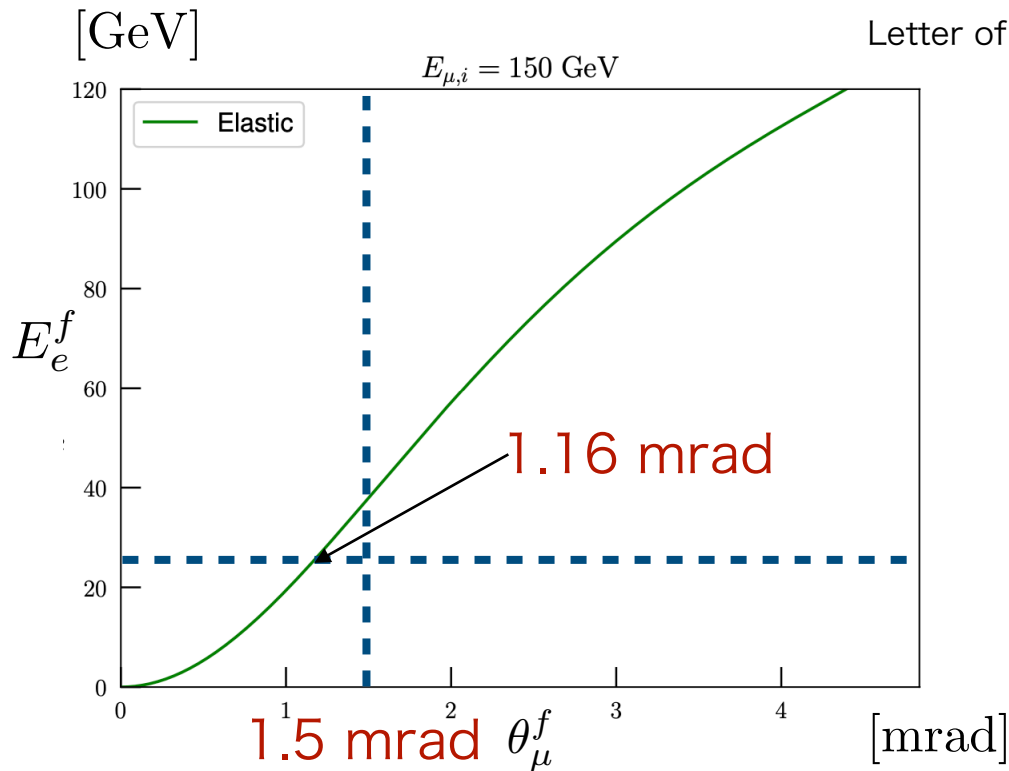


Fig. 10: Rms width of the δ_E distributions as a function of the electron energy, for electrons produced in the 1st (black), 5th (green), 10th (blue), 15th (red), and 20th (maroon) target. In the final apparatus, these stations correspond to 21st, 25th, 30th, 35th, and 40th.

MUonE sensitivity



tracker: Angular resolution: $O(0.01)$ mrad expected



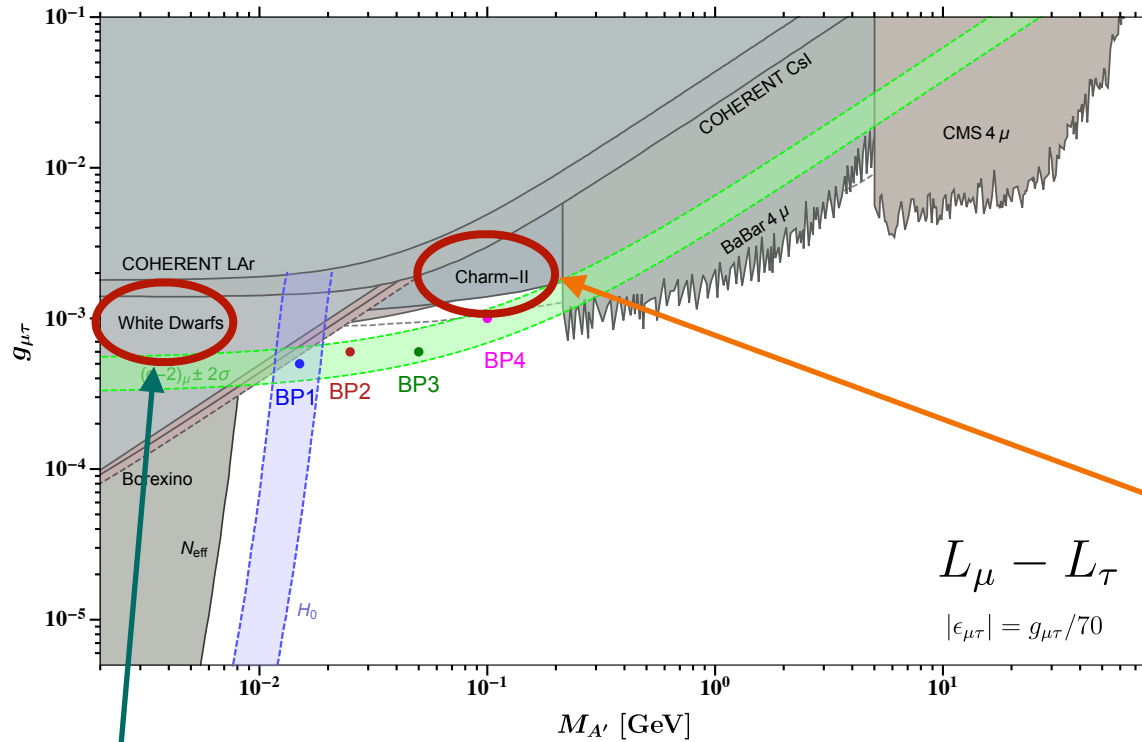
MUonE schedule

- ▶ Letter of Intent submitted in 2019.
- ▶ ~~Test run of 3 weeks is planned at the end of the running period of 2021.~~
- ▶ In 2021, parasitic run with one tracking station

Letter of Intent: <https://cds.cern.ch/record/2677471/files/SPSC-I-252.pdf>

C. Mussolini, et.al., JACoW IPAC2022 (2022) WEPOST024

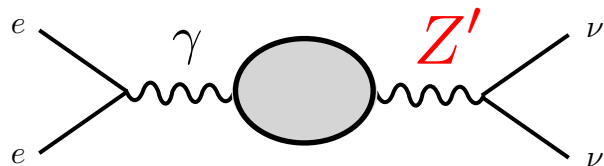
Other constraints



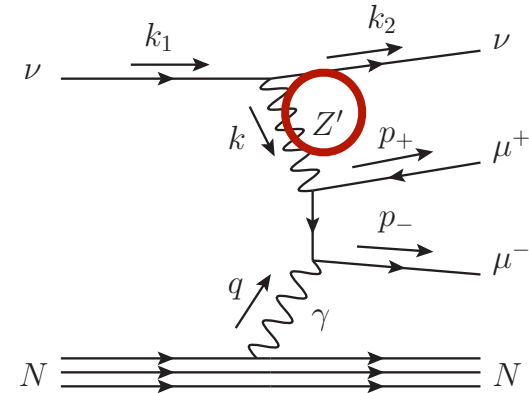
D.W.P. Amaral, et.al., Eur. Phys. J. C **81**, 861 (2021).

White dwarf cooling

M. Bauer, et.al., JHEP **07**, 094 (2018)



neutrino-trident process

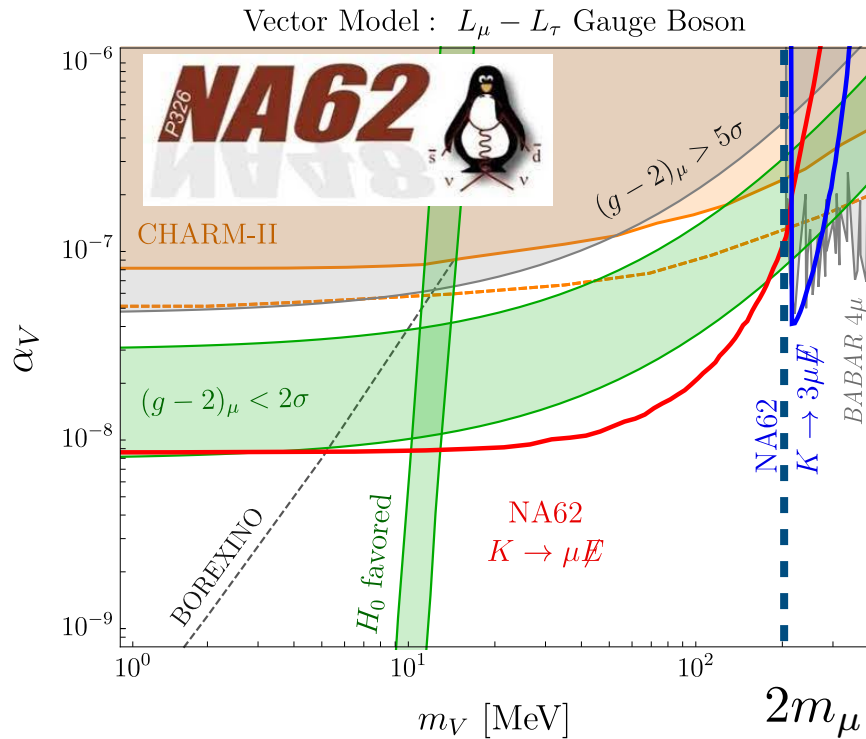


W. Altmannshofer, et.al., PRL. **113**, 091801 (2014)

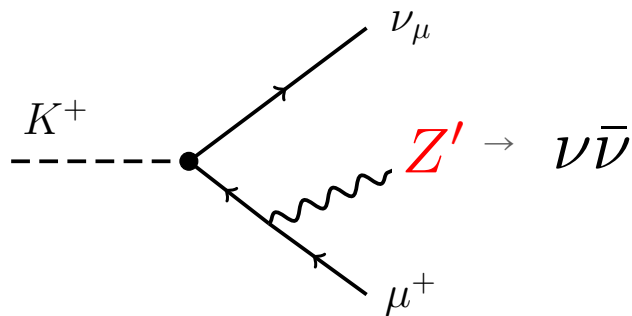
CHARM-II D. Geiregat et al. (CHARM-II),
Phys. Lett. B 245, 271 (1990).

CCFR S. R. Mishra et al. (CCFR),
Phys. Rev. Lett. 66, 3117 (1991).

Fate of g-2 region



G. Krnjaic, et.al., PRL. **124**, 041802 (2020)



The author assumed the full NA62 luminosity

$$N_{K^+} \approx 10^{13}$$

NA62 schedule

- Run1: 2016-2018
- Run2: 2021-2024

2021 NA62 Status Report to the CERN SPSC

cf)

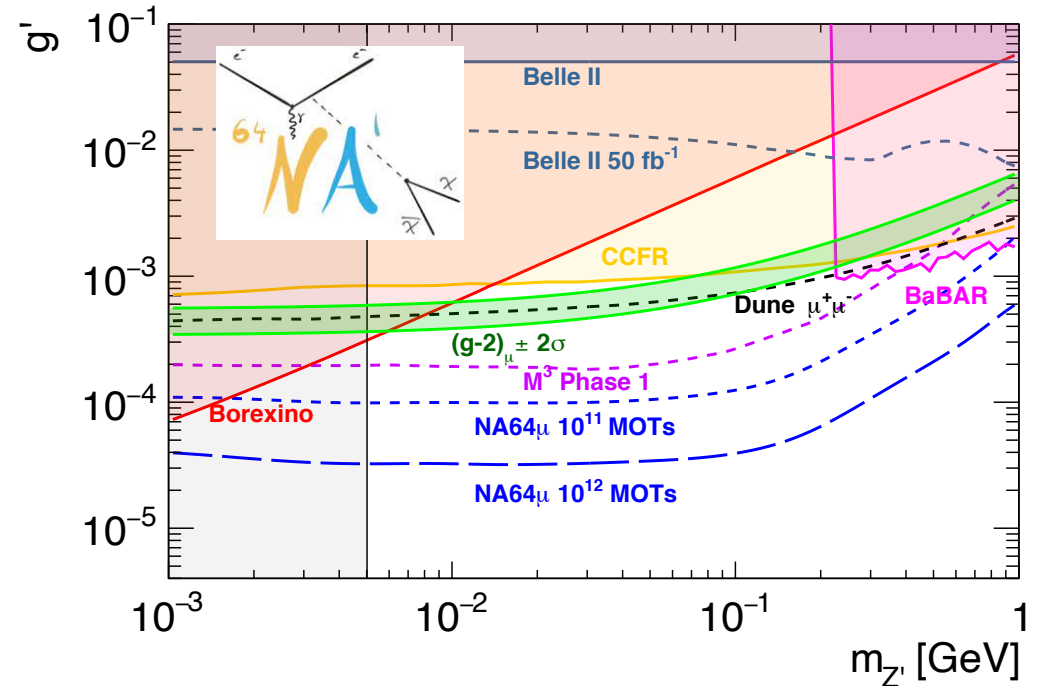
$$\text{Br}(K^+ \rightarrow \pi^+ \nu \bar{\nu}) \sim 10^{-11}$$

Fate of g-2 region

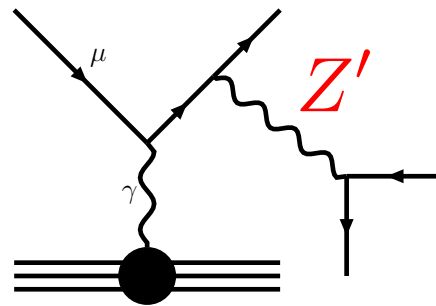
NA64 μ schedule

- ▶ Test run: 2021
 - ▶ Run1: 2022, 10^{11} MOT
- Final goal: 10^{13} MOT

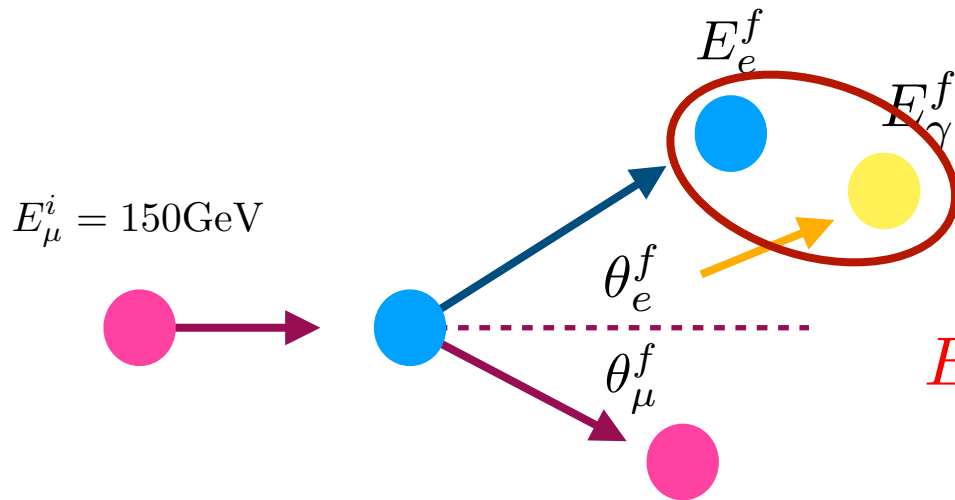
NA64 Status Report 2021



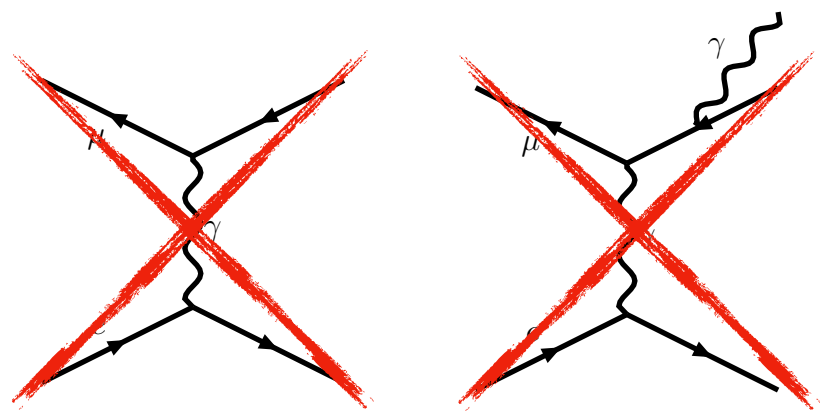
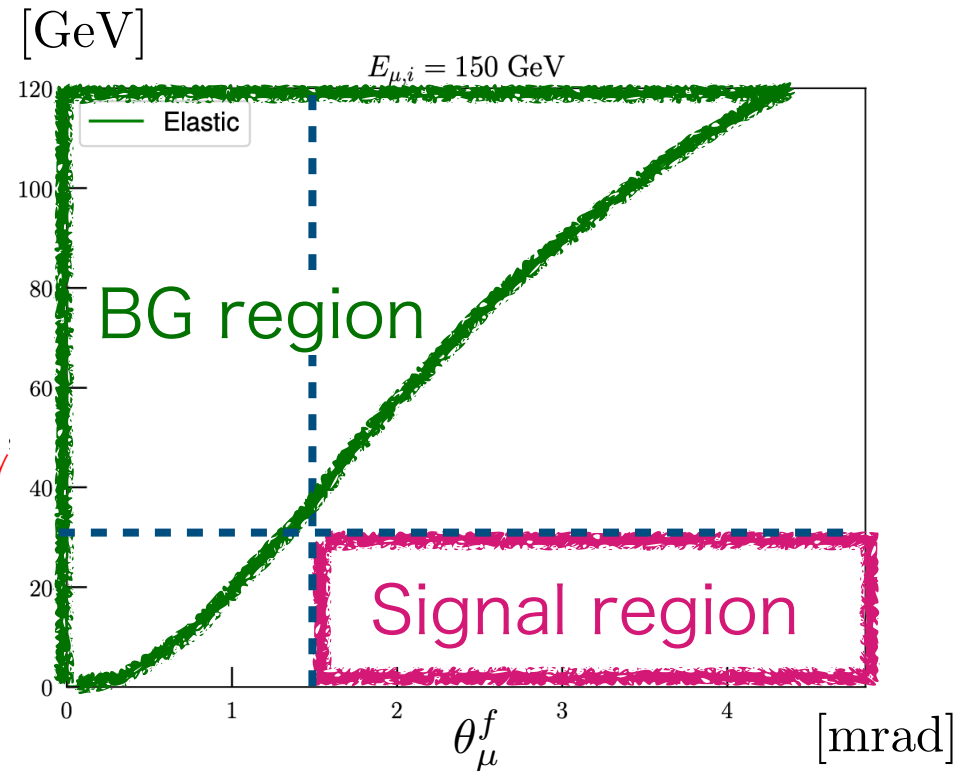
H. Sieber, et.al., 2110.15111



Strategy



$E_{e\gamma}^f$



▶ $\theta_{\mu}^f \geq 1.5 [\text{mrad}]$

▶ $E_e^f \leq 25 [\text{GeV}] \quad E_{e\gamma}^f \equiv E_e^f + E_{\gamma}^f$

$E_{e\gamma}^f$ is minimum when $E_{\gamma}^f \rightarrow 0$